Structural Properties and Surface Morphology of Magnesium Oxide Nanoparticles

[1] Zaw Win, [2] Soe Soe Oo*
[1] Technological University (Mandalay), Mandalay, Myanmar
[2] Technological University (Yamethin), Yamethin, Myanmar
drzawwin2015@gmail.com; drsoesoeoo2016@gmail.com

***Abstract*— The MgO nanoparticles were synthesized by a novel technique at very low temperature of 90 îC using de-ionized water as solvent and the synthesized particles were kept 600 îC for 30 minutes in the electrical furnace. The structural and morphological properties of MgO system were determined by using X-ray Diffraction (XRD) and Scanning Electron Micrographs (SEM) techniques. The results revealed that the as- prepared solids consisted entirely of well nano-crystalline magnesium oxide depending upon XRD data. X-ray diffraction analysis confirmed the formation of crystallite size and lattice constant in MgO powders having a single phase cubic structure. The crystallite size of the MgO sample has been measured from the Scherrer equation. The pore and grain microstructures have been studied by SEM. The MgO has a good bactericidal performance in aqueous environments.**

Keywords—MgO nanoparticles, X-ray Diffraction, Scanning Electron Micrographs, nano-crystalline, Scherrer equation, grain microstructures.

I. INTRODUCTION

Magnesium oxide (MgO) is a versatile metal oxide having numerous applications in many fields. It has been used as a catalyst and catalyst support for various organic reactions, as an adsorbent for removing dyes and heavy metals from wastewater, as an antimicrobial material, as an electrochemical biosensor and many other applications. Conventionally, MgO is obtained via thermal decomposition of various magnesium salts. The drawback with this method of obtaining MgO is the large crystallite size with low surface area-to-volume ratio that limits its applications for nanotechnology. Some properties of MgO, such as catalytic behaviour, can be further improved if it is used as nanosized particles compared to micron-sized particles. So, the formation of MgO nanostructures with a small crystallite size of less than 100 nm and homogeneous morphology has attracted much attention due to their unique physicochemical properties including high surface area-to-volume ratio. It is widely accepted that the properties of MgO nanostructures depend strongly on the synthesis methods and the processing conditions. Much effort has been devoted to synthesize MgO nanostructures using various methods such as precipitation, solvothermal, chemical vapour deposition, electrochemical, sonochemical, microwave, electron spinning, combustion, template and carbothermic reduction. Each method has its own advantages and disadvantages.

An important issue regarding synthesis and preparation of nanostructured MgO is controlling the parameters in order to obtain a more uniform size as well as morphology of the nanoparticles. Over the past decades, various starting materials were used in the synthesis methods producing nanosized MgO that may give multiple morphologies. Precursors that may be obtained from the synthesis methods may take many forms such as **magnesium hydroxide**, magnesium carbonate and basic magnesium carbonate.

Each precursor is annealed at a different temperature to produce highly crystalline and pure MgO. The advantages are its simplicity, cost-effectiveness, low reaction temperature, high surface area-to-volume ratio, narrow particle size distribution and high purity of the final product.

Early attempts to prepare magnesium oxalate dehydrate were by using either magnesium methoxide or magnesium ethoxide that was reacted with oxalic acid in ethanol to form a precursor based on the sol-gel reaction. Later on, inorganic salts like magnesium nitrate hexahydrate, magnesium chloride hexahydrate and magnesium acetate tetrahydrate are preferred. The sol-gel reaction of magnesium oxalate dihydrate and annealing of the obtained precursors give various morphologies of MgO nanostructures.

However, the controlled synthesis of MgO nanostructures with homogeneous morphology, small crystallite size and narrow size distribution is a challenging aspect to be investigated. Understanding the growth mechanism is an important part of controlling the size of nanostructures. The synthetic strategies of tailoring the size and shape of the nanostructures are key issues to be addressed in nanomaterials research [1].

To the best of our knowledge, there is no report on the effect of the molecular structure of complexing agents on MgO nanostructures even though the control of nanostructures presents an important part of nanotechnology work that is focused on the effect of complexing agents on the MgO nanostructures finally obtained after synthesis.

Compared with TiO_2, silver, copper and other kinds of solid bactericides, nano-MgO has the advantage of being prepared from readily available and economical precursors and solvents, and therefore has considerable potential as a solid bactericidal material under simple conditions. MgO uniform nanoparticles having diameters in the range of 50-70 nm were prepared by a simple reaction of magnesium hydroxide and de-ionized water at very low temperature of about 90 °C. The reported method, besides being simple, is non toxic, economical, fast, effective, and environmentally benign [2].

The aim of this research is to assess the structural and morphological properties of magnesium oxide. The employed techniques are X-ray diffraction (XRD) and scanning electron micrographs (SEM) techniques.

II. FUNDAMENTAL OF MATERIALS CHARACTERIZATION

A. X-ray Diffraction (XRD)

X-ray diffraction (XRD) is a powerful technique. It is the most widely used for the identification of unknown crystalline materials (eg- minerals, inorganic compounds). Other applications are the characterization of crystalline materials, identification of fine-grained materials such as clays and mixed layer clays that are difficult to determine optically, determination of unit cell dimensions and measurement of sample purity. XRD is also used to determine the thickness of thin films and multilayer and atomic arrangements in amorphous materials (including polymers) and at interfaces.

The specific wavelengths are characteristic of the target material (Cu, Fe, Mo, Cr). Copper is the most common target material for single-crystal diffraction, with CuK_{α} radiation. Filtering by foils or crystal monochromators, is required to produce monochromatic X-rays needed for diffraction. These X-rays are collimated and directed onto the sample. As the sample and detector are rotated, the intensity of the reflected X-ray is recorded.

When the geometry of the incident X-rays impinging the sample satisfies the Bragg equation, constructive interference occurs and peak intensity occurs (Figure 1). A detector records and processes this X-ray signal and converts the signal to a count rate which is then output to a device such as a printer or computer monitor. The geometry of an X-ray diffractometer is such as the sample rotates in the path of the collimated X-ray beam at an arm to collect the diffracted X-rays and rotates at an angle of 2θ. The instrument used to maintain the angle and rotate the sample is termed a goniometer. Figure 1 shows the basic features of an XRD experiment set up of the diffraction angle 2θ is the angle between the incident and diffracted X-rays. From 2θ values for reflection, 'd_{hkl}' values were calculated using Bragg equation and average crystallite size calculated of magnesium aluminate nanoparticles by Scherrer equation

$$D = \frac{0.9\,\lambda}{\beta \cos\theta}, \qquad (1)$$

where, D is the crystallite size, λ is the wavelength of the X-ray used, β is the full width at half maximum height and θ is the angle of diffraction. Crystals consist of planes of atoms spacing a distance d_{hkl} apart, but can be resolved into many atomic planes, each with a different d_{hkl} spacing.

When there is constructive interference from X-rays scattered by the atomic planes in a crystal, a diffraction peak is observed. The condition for constructive interference from planes with spacing d_{hkl} is given by Bragg's law:

$$\lambda = 2\, d_{hkl} \sin\theta, \qquad (2)$$

where, θ is the angle between the atomic planes and the incident and diffracted X-ray beam. For diffraction to be observed, the detector must be positioned so that the diffraction angle is 2θ, and the crystal must be oriented so that the normal to the diffracting plane is coplanar with the incident and diffracted [3,4,5].

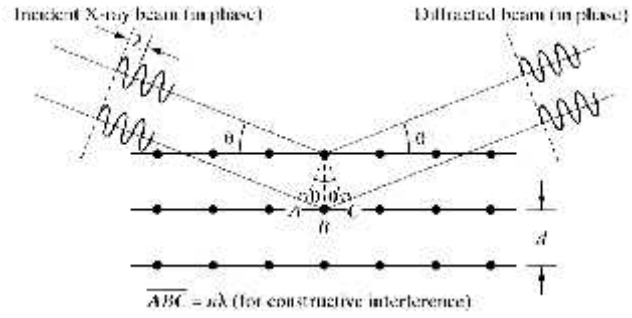

Figure 1. Reflection of crystal planes

B. Scanning Electron Microscope (SEM)

To observe the morphology of nanocomposites, a Scanning Electron Microscope model JEOL-JSM 5610 LV is used. It is a high-performance, low cost, scanning electron microscope with a high resolution of 3.0 nm. The scanning electron microscope (SEM) is a type of electron microscope that creates various images by focusing a high energy beam of electrons onto the surface of a sample and detecting signals from the interaction of the incident electrons with the sample's surface. The type of signals gathered in a SEM varies and can include secondary electrons, characteristic X-rays, and back scattered electrons. In a SEM, these signals come not only from the primary beam impinging upon the sample, but from other interactions within the sample near the surface. The SEM is capable of producing high-resolution images of a sample surface in its primary use mode, secondary electron imaging. Due to the manner in which this image is created, SEM images have great depth of field yielding a characteristic three-dimensional appearance useful for understanding the surface structure of a sample. This great depth of field and the wide range of magnifications are the most familiar imaging mode for specimens in the SEM. In the SEM, electrons from an electron source are accelerated to high energies and focused through a system of electromagnetic lenses onto the sample. In Figure 2, the focused electron beam is scanned across the sample surface, generating the different signal as illustrated. Characteristic X-rays are emitted when the primary beam causes the ejection of inner shell electrons from the sample and are used to tell the elemental composition of the sample. The back-scattered electrons emitted from the sample may be used alone to form an image or in conjunction with the characteristic X-rays as atomic number contrast clues to the elemental composition of the sample.

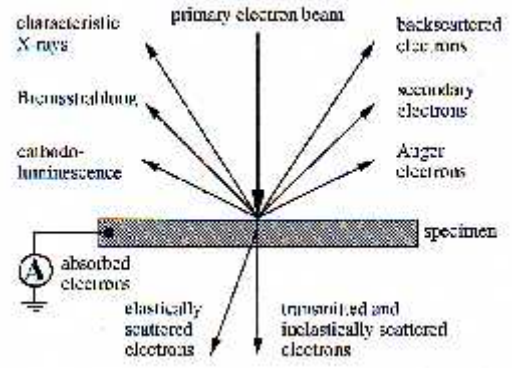

Figure 2. Schematic illustration of the incident electron beam generating different signals in the sample

The SEM provides a highly magnified image of the surface of a material that is very similar to what one would expect if one could actually "see" the surface visually. The resolution of the SEM can approach a few nanometer and it can operate at magnifications that are easily adjusted from about 10X – 300,000X.

In the SEM, a source of electrons is focused (in vacuum) into a fine probe that is rastered over the surface of the specimen. As the electrons penetrate the surface, a number of interactions occur that can result in the emission of electrons or photons from (or through) the surface. A reasonable fraction of the electrons emitted can be collected by appropriate detectors, and the output can be used to modulate the brightness of a cathode ray tube (CRT) whose x- and y-inputs are driven in synchronism with the x-y voltages rastering the electron beam. In this way an image is produced on the CRT; every point that the beam strikes on the sample is mapped directly onto a corresponding point on the screen.

If the amplitude of the saw-tooth voltage applied to the x- and y-deflection amplifiers in the SEM is reduced by some factor while the CRT saw-tooth voltage is kept fixed at the level necessary to produce a full screen display, the magnification, as viewed on the screen, will be increased by the same factor [3,4,5].

III. Sample Preparation

In this research, 0.102 g of magnesium hydroxide was taken in a vial containing 500 ml of de-ionized water and was well stirred for 2 hours. And then, the solution was heated in oven at 90 °C for 9 hours. The precipitated solution was filtered with filter paper to reclaim the precipitated sample and it was washed with distilled water and dried in air for 24 hours. Finally, the dried powders were calcined at temperatures of 150 °C and 600 °C for 2 hours and 30 minutes in electrical furnace. After that the system was naturally cooled to room temperature and the final white powder was obtained. The sample preparation flow chart was described in Figure 3. Figures 4 to 9 illustrate the sample preparation procedures.

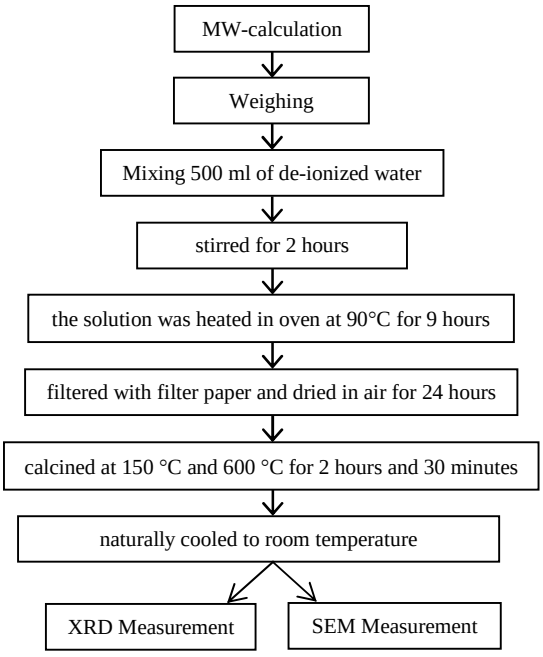

Figure 3. Sample preparation flow chart

Figure 4. Weighing the raw sample with digital balance

Figure 5. Stirring the raw sample with magnetic stirrer

Figure 6. Heating the mixture in an oven

Figure 7. Filtering the precipitated sample

Figure 8. Calcinating the precipitated sample

Figure 9. Coating for SEM measurement

IV. Results and Discussion

Firstly, the raw material of $Mg(OH)_2$ powder was analyzed by X-ray diffractometer to check if it was pure magnesium hydroxide. The results of XRD pattern was shown in Figure 10. Study of this figure revealed that the raw material was slightly soluable-powder, $Mg(OH)_2$, depending upon PDF2 card No. 44- 1482. Various planes (0 0 1), (1 0 1), (1 0 2) and (1 1 0) have been determined. The X-ray diffraction measurement showed that all peaks are consistent with those of $Mg(OH)_2$ powder having a hexagonal structure.

In Figure 11, the XRD pattern for $Mg(OH)_2$ was calcined at 150˚C for 2 hours in an oven. Study revealed that the as synthesized sample could not reach the target result, MgO. But there was mixed patterns of MgO and $Mg(OH)_2$. Therefore, the sample was required to give higher temperature than 150 °C to approach target result magnesium oxide, MgO.

Figure 12 shows the XRD pattern for MgO (calcined at 600 ˚C for 30 minutes) sample. Depending upon PDF2 card No. 44- 1482, study revealed that the as synthesized sample consisted some part of magnesium hydroxide, $Mg(OH)_2$, particles. But it was cleared that the sample was mostly transformed into MgO nanoparticles analyzed by XRD pattern. The planes of MgO, (1 1 1), (2 0 0) and (2 2 0), were determined by PDF2 card No. 77-2179. These planes are relative to the cubic structure, space group *Fm3m [225]*, of magnesium oxide. Peaks Comparison for MgO are described in Figure 13.

The calculated values of the (d_{hkl}) spacings, lattice constants (a_0), unit cell volumes (V) and X-ray density (D_x) of MgO nano- particles depending upon the data of X-ray are given in Table I.

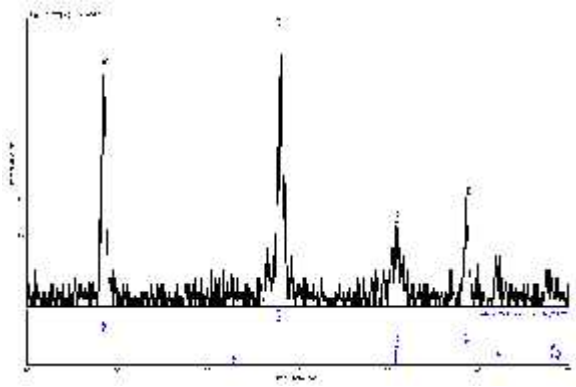

Figure 10. XRD pattern of $Mg(OH)_2$ raw material

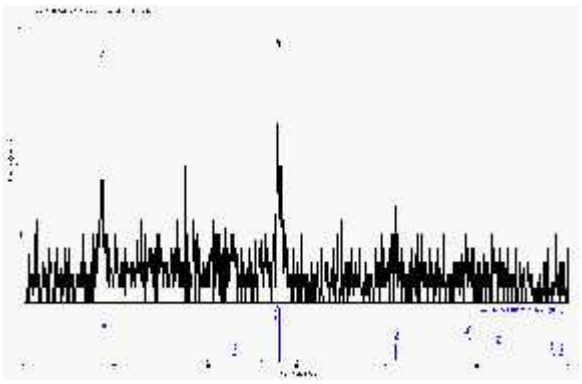

Figure 11. XRD pattern of $Mg(OH)_2$ calcined at 150 °C for 2 hours

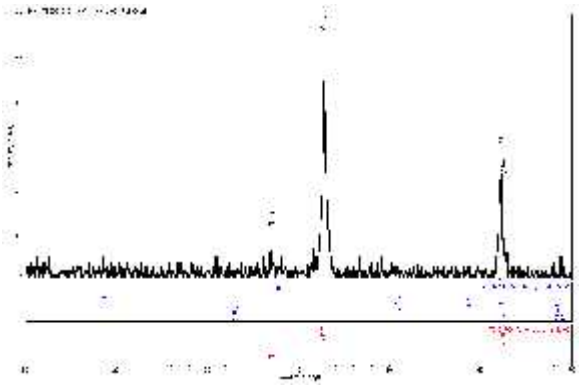

Figure 12. XRD pattern of MgO calcined at 600˚C for 30 min

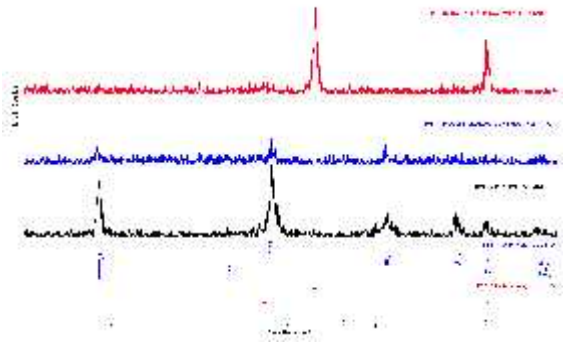

Figure 13. Peaks Comparison for MgO at various temperatures

The crystallite size of the synthesized samples was calculated by using the peak width at half intensity of the three peaks (111), (200) and (220) in Scherrer's equation. The crystallite sizes are about 83.75 nm, 23.57 nm and 22.25 nm which are shown in Table II. They are mostly in good agreement with the other data [6,7,8,9].

Table I. Some Structural Parameters for the As-Prepared MgO System at 600 °C

(hkl)	d_{hkl} (Å)	*a* (Å)	*V* (Å^3)	D_x (g/cm^3)
(111)	2.4305	4.2098	74.608	3.5835
(200)	2.1086	4.2173	75.007	3.5835
(220)	1.4869	4.2056	74.385	3.5835

Table II. Crystallite Size Calculation for MgO at 600 °C

(hkl)	2^-	cos^-	(FWHM)	^{a}- (Å)	*D* (nm)
(111)	36.954	0.9484	0.1	1.54056	83.75
(200)	42.852	0.9309	0.362	1.54056	23.57
(220)	62.402	0.8553	0.417	1.54056	22.25

The microstructure of the as-prepared sample was shown in Figure 14. SEM images give information about the intergranular and intragranular pores as well as the sub-structural defects within the grains. MgO sample was characterized by small grain and porosity. The surface morphology of the sample as seen from the SEM photograph consists of grain varying from 2 µm to 5 µm.

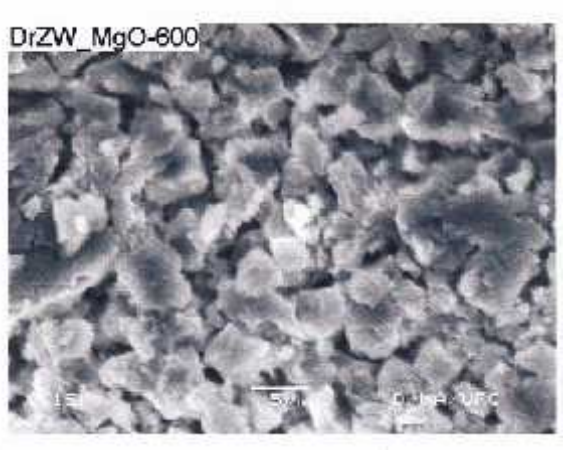

Figure 14. Scanning electron micrograph of MgO

V. Conclusion

The MgO nanoparticles were successfully prepared by using a novel technique at very low temperature of 90˚C using de-ionized water as solvent. The endothermic decomposition undergoes at 600 °C: $Mg(OH)_2 \rightarrow MgO + H_2O$ in this research. The values of d_{hkl} spacing, lattice parameter, volume and X-ray density of MgO nanoparticles were determined. XRD analysis clearly revealed that the crystallite sizes are found to be 83.75 nm, 23.57 nm and 22.25 nm respectively. The smaller the grain sizes the more smoothness the surface is. The planes of MgO, (1 1 1), (2 0 0) and (2 2 0) have been determined by PDF2 card No. 77-2179. These planes are relative to the cubic structure of magnesium oxide with space group *Fm3m [225]*. The surface morphology of the sample was determined by using the SEM photograph consisting of grain size varying from 2 µm to 5 µm. The grain size decreases with increasing temperature. So, MgO has a good bactericidal performance and considerable potential in aqueous environments under simple conditions.

Acknowledgments

We would like to express our special thanks to Pro-Rector, Technological University (Bamaw) for accepting this research paper.

Next, we are grateful to our reviewers for their comments.

Finally, we thank our colleagues at Universities' Research Centre, University of Yangon for the uses of their facilities.

References

[1] M. S. Mastuli et al., "Growth Mechanism of MgO Nanocrystals via a Sol-Gel Synthesis Using Different Complexing Agents," *Nanoscale Research Letters*, vol. 9, no. 134, pp. 1-9, 2014.

[2] M. A. Shah, "Preparation of MgO Nanoparticles with Water," *African Physical Review*, vol. 4, no. 4, pp. 21-23, 2010.

[3] Aye Aye Thant, Pho Kaung, S. Srimala, M. Itoh, R. Othman, and M. N. Fauzi, "Proceedings of the PSU-UNS International Conference on Engineering & Environment (ICEE 2007), Thailand," 2007.

[4] C. Kittle, "Introduction to Solid State Physics," New York: Wiley, 2005.

[5] Ei Zar Tun, "Structure and Surface Morphology of Mg-Cu Ferrite Material," M.Res. Thesis, Taungoo University, March 2017.

[6] M. A. Karimi et al., "Synthesis and Characterization of Nanoparticles and Nanocomposite of ZnO and MgO by Sonochemical Method and Their Application for Zinc Polycarboxylate Dental Cement Preparation," *Int. Nano Lett.*, vol. 1, no. 1, pp. 43-51, 2011.

[7] M. Ajmal and A. Maqsood, "Influence of Zinc Substitution on Structural and Electrical Properties of $Ni_{1-x}Zn_xFe_2O_4$ Ferrites," *Mater. Sci. Eng. B*, vol. 139, Issues 2-3, pp. 164-170, May 2007.

[8] Rizwan Wahab et al., "Synthesis of Magnesium Oxide Nanoparticles by Sol-Gel Process," *Materials Science Forum*, vol. 558, pp. 983-986, 2007.

[9] P. Tamilselvi et al., "Synthesis of Hierarchical Structured MgO by Sol-Gel Method," *Nano Bulletin*, vol. 2, no. 1, 130106-1, 2013.